Superlattices and Microstructures 33 (2003) 155–171

Superlattices and Microstructures

www.elsevier.com/locate/jnlabr/yspmi

Phonon spectrum and group velocities in AlN/GaN/AlN and related heterostructures

Evghenii P. Pokatilov[a], Denis L. Nika[a], Alexander A. Balandin[b,*]

[a] *Department of Theoretical Physics, State University of Moldova, Kishinev, Moldova*
[b] *Nano-Device Laboratory, Department of Electrical Engineering, University of California - Riverside, Riverside, CA 92521, USA*

Received 7 July 2003; accepted 24 July 2003

Abstract

We theoretically investigated acoustic phonon spectrum and group velocities in an ultra-thin layer of wurtzite GaN embedded within two AlN cladding layers. The core GaN layer thickness has been chosen on the order of the room-temperature dominant phonon wavelength so that the phonon spectrum in such a structure is strongly modified compared to bulk. We derived equations of motion for different phonon polarizations in the anisotropic medium approximation, which allowed us to include specifics of the wurtzite lattice. Based on our model we calculated phonon density of states and phonon group velocity. Using several other example material systems, it has also been demonstrated that the phonon group velocity in the core layer can be made higher or lower than that in corresponding bulk material by a proper selection of the cladding material and its thickness. Presented results shed new light on the effect of barrier material on the phonon spectrum of heterostructures and can be used for modeling the thermal and electrical properties of such structures.

1. Introduction

Acoustic phonons play an important role in electrical and thermal properties of semiconductor materials. Together with optical phonons they limit room-temperature electron (hole) mobility of technologically important semiconductors such as Si, GaAs or GaN. Acoustic phonons are dominant heat carriers in moderately doped semiconductors in a wide range of temperatures from cryogenic to almost the melting point [1]. Acoustic phonons in bulk semiconductors are characterized by a nearly linear dispersion relation

* Corresponding author.
E-mail address: alexb@ee.ucr.edu (A.A. Balandin).

0749-6036/$ - see front matter © 2003 Elsevier Ltd. All rights reserved.
doi:10.1016/S0749-6036(03)00069-7

near the Brillouin zone center, wide continuous spectral range and high population densities even at low temperature. In semiconductor heterostructures and nanostructures with feature size W smaller than the phonon mean free path Λ, the acoustic phonon spectrum can undergo strong modification and appear quantized provided the structures are free standing or embedded within material of different elastic properties [2]. This modification is particularly strong when the structure feature size becomes much smaller than the phonon mean free path, $W \ll \Lambda$, and approaches the scale of the dominant phonon wavelength $\lambda_d \cong 1,48 V_S \hbar / k_B T$ [3]. Here k_B is the Boltzmann constant, T is the absolute temperature, $\hbar$ is Plank's constant, and V_S is the sound velocity. This scale for many crystalline materials is on the order of a nanometer at room temperature.

Quantization of acoustic phonons, much like quantization of electrons (holes) affects electrical, optical and thermal properties of ultra-thin films and nanostructures. The signatures of phonon quantization can be found in radiational and non-radiational relaxation of electrons [4–6], phonon bottleneck effect [7, 8] and stimulated far-infrared emission from quantum dots [9]. More recently it has been shown theoretically that confinement-induced modification of the acoustic phonon spectrum in free-surface ultra-thin films [2] and nanowires [10–12] leads to a significant decrease of the in-plane lattice thermal conductivity even at room temperature. The decrease of thermal conductivity due to phonon confinement may bear important consequences for the electronic industry in a view of continuous miniaturization. The feature size of the state-of-art transistor is already on the order of or below the room-temperature phonon mean free path. In some applications, such as thermoelectrics, smaller thermal conductivity is strongly desirable. These two facts stimulated a large body of work on phonons in heterostructures and nanostructures. Intentional modification of the phonon spectrum to achieve enhanced device performance has been termed phonon engineering.

The investigation of acoustic phonon spectra in the context of semiconductor structures dates back to as early as half a century ago. A nomenclature of analytical results for free standing slabs can be found, for example, in [13]. Theoretically, the folded acoustic phonons in layered medium have been studied by Rytov [14]. Later, the folded phonons have been observed experimentally in quantum well superlattices (QWS) [15]. Many theoretical results for quantized phonons in free standing films, nanowires and spherical quantum dots were obtained using the analogy with acoustics and classical mechanics [16–18]. Dispersion of dilatational, flexural and shear vibrational modes in thin films has been described in [16], dispersion of hybrid thickness and width modes has been obtained in [17]. More recently, phonon dispersion in quantum dot superlattices (QDS) has been calculated taking into account elastic constants of both dot and barrier material [19]. The above cited results for confined phonons in thin films and nanowires were obtained under the assumption of the free surface, e.g. free standing, or clamped surface boundary conditions [16–18]. In the core of electronic and optoelectronic devices are multilayered structures made of materials, which are rather similar in terms of elastic properties. Thus, the assumption of free or clamped surface boundary is rather crude for such device structures.

The important question for phonon transport in the plane of a thin film or along the axis of a nanowire, which has not been properly addressed yet, is the effect of the surrounding material (matrix, barrier, or cladding) on acoustic phonon spectra of ultra-thin

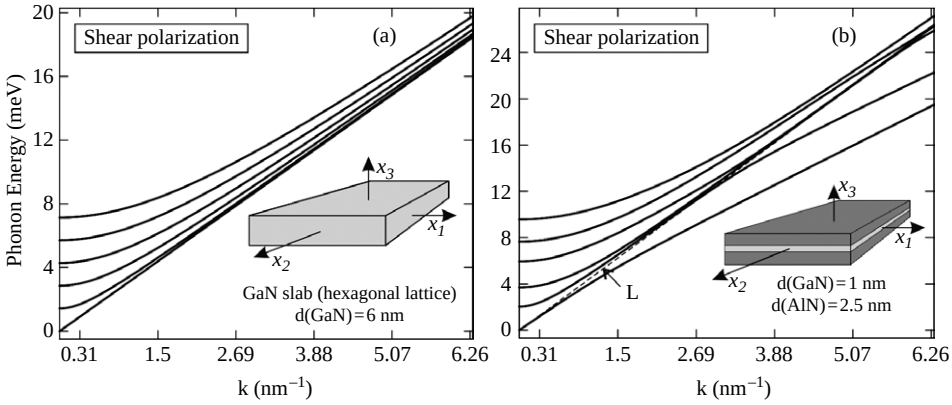

Fig. 1. Phonon energies as the functions of the phonon wavevector for the shear polarization for (a) a 6 nm width semiconductor GaN slab and for (b) a AlN/GaN/AlN three-layered heterostructure with dimensions 2.5/1/2.5 nm. Insets show the slab geometry and coordinate system.

films and heterostructures. In this paper we address this issue and investigate the acoustic phonon spectrum of a three-layered semiconductor structure with ultra-thin inside layer and cladding (barrier) material made of a "harder" or "softer" semiconductor. We carry out our calculations for wurtzite AlN/GaN/AlN heterostructures and several other related heterostructures in order to elucidate the effect of "hard" and "soft" cladding material. The rest of the paper is organized as follows. In Section 2 we derive the equations of motion for the elastic vibrations in the three-layered structure. Results and discussion are presented in Section 3. We give our conclusions in Section 4.

2. Theoretical model

In order to investigate the role of the cladding material on the acoustic phonon spectrum of ultra-thin films we consider a free-standing single thin film, e.g. slab, and a free-standing three-layered structure, e.g. double heterostructure. Both structures have a nanometer feature size along the growth direction. A schematic view of the slab and three-layered structure are shown in the insets to Fig. 1(a, b). The axes X_1 and X_2 in the Cartesian coordinate system are in the plane of the layers while the axis X_3 is directed perpendicular to the layer surfaces. The layer thickness is denoted by $d_i (i = 1, 2, 3)$. As an example system we first consider the AlN/GaN/AlN heterostructure. GaN and related compounds crystallize in the wurtzite (hexagonal) or zincblende (cubic) lattice. Here we limit our analysis to wurtzite GaN as it is technologically more important. It is further assumed that the layers have hexagonal symmetry with a crystallographic axis c directed along a coordinate axis X_3.

The equation of motion for elastic vibrations in an anisotropic medium can be written as

$$\rho \frac{\partial^2 U_m}{\partial t^2} = \frac{\partial \sigma_{mi}}{\partial x_i}, \tag{1}$$

where $\vec{U}(U_1, U_2, U_3)$ is the displacement vector, ρ is the mass density of the material, σ_{mi} is the elastic stress tensor given by $\sigma_{mi} = c_{mikj}U_{kj}$, and $U_{kj} = (1/2)((\partial U_k/\partial x_j) + (\partial U_j/\partial x_k))$ is the strain tensor. The normal acoustic modes in multilayer structures and superlattices have been studied by Rytov [14] in homogeneous ($c_{iklm} = \text{const}$) and isotropic medium approximation by enforcing the boundary conditions on all interfaces of the structures.

In this paper we modify the form of the boundary conditions to make them more convenient for numerical solution for a multi-layered wurtzite heterostructure. When taking derivatives in Eq. (1), one has to take into account that the system is non-uniform along the X_3 axis. The elastic modules are the piece-wise functions of x_3:

$$c_{mikj} = c_{mikj}(x_3). \tag{2}$$

To reduce the number of subscript indexes in the coefficients c_{mikj}, we adopt the two-index notations according to the prescription

$$1111 \to 11;\ 2222 \to 22;\ 3333 \to 33;\ 1122 \to 12;\ 1133 \to 13;\ 1313 \to 44;$$
$$2323 \to 55;\ 1212 \to 66.$$

In crystals with hexagonal symmetry the following equalities are valid:

$$c_{1313} = c_{2323} = c_{44};\ c_{1212} = c_{66} \neq c_{44}. \tag{3}$$

Thus, we have six independent elastic constants to characterize the material. An application of the anisotropic continuum model allows us to explicitly include the specifics of lattice structure of wurtzite crystals. The equations of motion obtained in anisotropic medium approximation with such a selection of the elastic constants will be completely different from the equations of motion in the isotropic elastic medium approximation or anisotropic medium approximation for cubic crystals.

The axis X_1 is assumed to be along the propagation direction of the acoustic waves. Since the three-layered structure is homogeneous in the plane (X_1, X_2), we look for the solution of the Eq. (1) in the following form

$$U_i(x_1, x_3, t) = u_i(x_3)\mathrm{e}^{\mathrm{i}(\omega t - kx_1)} \qquad (i = 1, 2, 3), \tag{4}$$

where u_i are the amplitudes of the displacement vector components, ω is the phonon frequency, k is the phonon wavevector and $\mathbf{i}$ is imaginary unit.

A shear polarization, e.g. the displacement vector is parallel to the structure surfaces, can be distinguished from the others using the following definition

$$\rho\frac{\partial^2 U_2}{\partial t^2} = \frac{\partial \sigma_{2i}}{\partial x_i}. \tag{5}$$

By substituting Eq. (4) for $i = 2$ to Eq. (5) and taking into account Eqs. (2) and (3), one can turn the partial differential equation (5) into an ordinary second order differential equation

$$-\rho\omega^2 u_2(x_3) = c_{44}\frac{\mathrm{d}^2 u_2(x_3)}{\mathrm{d}x_3^2} + \frac{\mathrm{d}c_{44}}{\mathrm{d}x_3}\cdot\frac{\mathrm{d}u_2(x_3)}{\mathrm{d}x_3} - c_{66}k^2 u_2(x_3). \tag{6}$$

Derivatives dc_{ik}/dx_3 account for the fact that the structure is heterogeneous. In the case of a slab, one can obtain a simple analytical solution from Eq. (6) by setting $dc_{44}/dx_3 = 0$ (see, for example [13, 16]). The external surfaces of the three-layered structure are assumed to be free. As a result, the force components along all coordinate axes are equal to zero, e.g. $P_1 = P_2 = P_3 = 0$ where $P_i = \sigma_{ik} n_k$ and $\vec{n}$ is the vector normal to the surfaces of the structure $\vec{n} = (0, 0, n_3)$. Thus, on the outer surfaces of the structure the following relationship is satisfied

$$\frac{\partial u_2}{\partial x_3} = 0. \tag{7}$$

For the two other vibrational polarizations ($i = 1, 3$) with the displacement vector components U_1 and $U_3' = -\mathbf{i}U_3$ we obtain the system of two interrelated equations using Eqs. (1) and (4). These equations are given as

$$-\rho\omega^2 u_1(x_3) = -k^2 c_{11} u_1(x_3) + c_{44}\frac{d^2 u_1(x_3)}{dx_3^2} + k(c_{13} + c_{44})\frac{du_3'(x_3)}{dx_3} + \frac{dc_{44}}{dx_3}\left(\frac{du_1(x_3)}{dx_3} + k u_3'(x_3)\right), \tag{8}$$

$$-\rho\omega^2 u_3'(x_3) = -k^2 c_{44} u_3'(x_3) + c_{33}\frac{d^2 u_3'(x_3)}{dx_3^2} + \frac{dc_{33}}{dx_3}\frac{du_3'(x_3)}{dx_3} - k\left[(c_{44} + c_{13})\frac{du_1(x_3)}{dx_3} + \frac{dc_{13}}{dx_3}u_1(x_3)\right], \tag{9}$$

with the following boundary conditions on the outer surfaces of the structure

$$\frac{du_1}{dx_3} + k u_3' = 0, \qquad -k c_{13} u_1 + c_{33}\frac{du_3'}{dx_3} = 0. \tag{10}$$

Due to the spatial symmetry of the considered three-layered structure and the mathematical form of Eqs. (8) and (9), the displacement vector should have components with an opposite parity, e.g. $(u_1^{\mathrm{S}}, u_3^{\mathrm{A}})$ or $(u_1^{\mathrm{A}}, u_3^{\mathrm{S}})$, where $u_i^{\mathrm{S}}(x_3)(i = 1, 3)$ is a symmetrical function of x_3 while $u_i^{\mathrm{A}}(x_3)$ $(i = 1, 3)$ is an anti-symmetrical function of x_3. The upper indexes SA and AS of displacement vectors $\vec{u}^{\mathrm{SA}} = \vec{u}(u_1^{\mathrm{S}}, u_3^{\mathrm{A}})$ and $\vec{u}^{\mathrm{AS}} = \vec{u}(u_1^{\mathrm{A}}, u_3^{\mathrm{S}})$ distinguish independent vibrational polarizations which, together with the shear modes, compose a full set of normal vibrational modes in the structure. In the case of a slab the SA modes are referred to as dilatational modes while AS modes are termed the flexural modes [13, 14, 16, 17].

3. Results and discussion

To obtain the vibrational spectrum, e.g. phonon dispersion, of the three-layered structure we solve the differential equation (6) with the boundary condition of Eq. (7) for shear polarization, and the system of Eqs. (8) and (9) subject to the boundary conditions of Eq. (10) for SA and AS polarizations. The equations are solved using the finite difference method. The calculations are performed for each value of the phonon

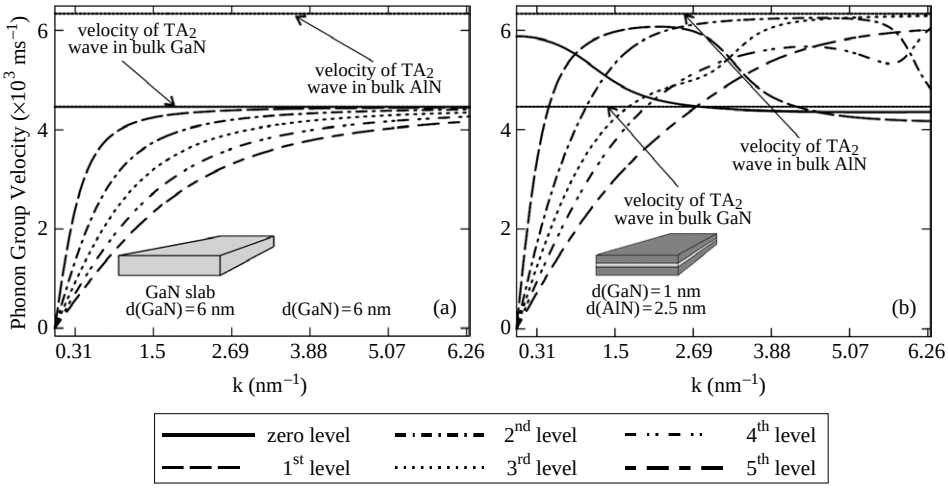

Fig. 2. Phonon group velocities as the functions of the phonon wavevector for the shear polarization. Results are shown for (a) a 6 nm width semiconductor GaN slab and for (b) a AlN/GaN/AlN three-layered heterostructure with dimensions 2.5/1/2.5 nm.

wavevector k from the interval $k \in (0, \pi/a)$, where a is the lattice constant in the plane (X_1, X_2). Since we are interested in the properties of ultra-thin films (quantum wells), we assume that the structure is non-relaxed and, thus, the lattice constant is the same for both the thin film and barrier materials. The phonon dispersion is calculated for all three polarizations: shear, SA and AS. Material parameters used in our simulations have been taken from [20–23].

3.1. Phonon modes in ultra-thin GaN layer embedded within AlN cladding layers

The characteristic features of the phonon dispersion relations can be easily seen on the plots of the phonon group velocity as a function of the wavevector k, which is given as

$$v_n^{\mathrm{SA,AS,sh}}(k) = \frac{\mathrm{d}}{\mathrm{d}k}\omega_n^{\mathrm{SA,AS,sh}}(k). \tag{11}$$

Here the superscript denotes the polarization type, while the subscript n is the quantum number of the modes with a given polarization. Using the above expression we then calculate the group velocity for each mode.

First, we consider phonon modes of the shear polarization, for which the effects of quantization and the system heterogeneity are exhibited in a more pronounced way than those for SA and AS polarizations. Fig. 1(a, b) and Fig. 2(a, b) show the dispersion relation $\hbar\omega_n^{\mathrm{sh}}(k)$ and the group velocity $v_n^{\mathrm{sh}}(k)$ for a set of shear modes. Figs 1(a) and 2(a) present data for a GaN slab with thickness $d = 6$ nm. Figs 1(b) and 2(b) present data for a three-layered AlN/GaN/AlN with dimensions 2.5/1/2.5 nm. For the convenience of further discussion, we refer to such a heterostructure as a type-I structure to emphasize that the cladding layers are thicker than the core layer. One can see from Fig. 1 that near the

Brillouin zone center (small values of k) the phonon modes are quantized and the modes with $n \neq 0$ are quadratically dispersive. In the zone center the phonon group velocity is a linear function of the phonon wavevector $v_n^{\mathrm{sh}}(k) = a_n k$ (see Fig. 2(a)).

With increasing k all dispersion curves approach a limit $\hbar\omega_0(k) = v_0\hbar k$, where $v_0 = v^{\mathrm{TA}_2}(\mathrm{GaN})$ and v^{TA_2} is the velocity of the transverse acoustic wave propagating along the X_1 axis and polarized along the X_2 axis (TA_2 polarized waves). The mode with $n = 0$ is bulk-like for all values of k. For large values of k (see Fig. 1(a, b)) modes with $n \neq 0$ also become GaN bulk-like. Note, that in the case of the clamped surface boundary conditions the zero bulk-like mode vanishes. Strong size-quantization of phonon spectra for small values of k, emergence of quasi-optical modes and significant decrease of the phonon group velocity ($v_n(k) < v^{\mathrm{TA}_2}(\mathrm{GaN})$) constitute the phonon confinement effects in an ultra-thin slab. These effects were shown to have a pronounced influence on the lattice (phonon) thermal conductivity of semiconductor quantum wells [2].

The inhomogeneity of the three-layered structure changes the shape of the dispersion curves both quantitatively and qualitatively (compare panels (a) and (b) in Figs 1 and 2). The steep segments of each of the dispersion curves in Fig. 1(b) distinguish these curves from the monotonic dispersion curves of Fig. 1(a). These segments are arranged in order of increasing mode number n and can be joined together by a straight line, which is indicated in Fig. 1(b) by the symbol "L". One can also define a characteristic velocity as $\hbar\omega_{\mathrm{L}}(k) = v_{\mathrm{L}}\hbar k$. As one can see from Fig. 2(b), the phonon group velocities on these segments coincide approximately with the velocities of TA_2 bulk phonons in AlN. Thus, on a straight line L the phonon modes are (AlN, TA_2) bulk-like.

The dispersion curves to the left and above the line L appear to look like dispersion curves in a slab. This region of strong phonon size-quantization is qualitatively similar for all considered structures and polarizations. The modes with small n and large phonon wavevector k split off down from line L and are (GaN, TA_2) bulk-type. For large n at large k the phonon modes are (AlN, TA_2) bulk-type (see Fig. 2(b)). The phonon modes in the multi-layered structure are formed as a result of superposition of vibrations from different layers on the structure interfaces, which leads to the mode hybridization. It is interesting to note, that depending on the k value the hybrid modes can reveal signatures of the specific layers rather then those of the averaged structure properties. For example, the group velocity for the mode with $n = 1$ at moderate k is $v^{\mathrm{TA}_2}(\mathrm{AlN})$, while at large k the group velocity is $v^{\mathrm{TA}_2}(\mathrm{GaN})$, although the total width of the cladding AlN layers is five times larger than the width of the core GaN layer. The group velocity of the mode $n = 5$ tends monotonically to the bulk velocity $v^{\mathrm{TA}_2}(\mathrm{AlN})$. Fig. 3 illustrates "retraction" of the mode $n = 0$ to the "soft" core GaN layer from the "hard" AlN cladding layer as the phonon wavevector k increases. As a result the group velocity of this mode changes from $v = v^{\mathrm{TA}_2}(\mathrm{AlN})$ at small k to $v = v^{\mathrm{TA}_2}(\mathrm{GaN})$ for large k.

In Figs 4(a–d) and 5(a–d) we present the evolution of the phonon dispersion and group velocity for SA (solid line) and AS (dashed line) modes in a three-layered structure when the core layer width increases from 0 nm (AlN slab (Figs 4(a), 5(a))) to 6 nm (GaN slab (Figs 4(d), 5(d))). One can notice in Fig. 4(a, d) that the characteristic line L can be identified for the slab SA and AS modes whereas it is absent for the shear slab modes shown in Fig. 1(a). The slope v_{L} of the line L is approximately equal to $v^{\mathrm{LA}}(\mathrm{AlN})$, where v^{LA} is the velocity of the longitudinal acoustic wave propagating along X_1 (LA polarized waves).

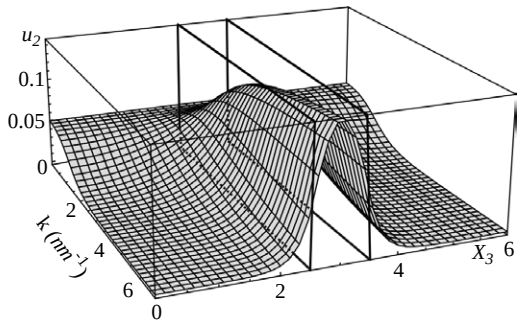

Fig. 3. Dependence of the normalized amplitude $u_2(x_3)$ on the wavevector k in the type-I heterostructure. Outer parallelepipeds correspond to AlN cladding layers while interior parallelepiped corresponds to GaN core layer.

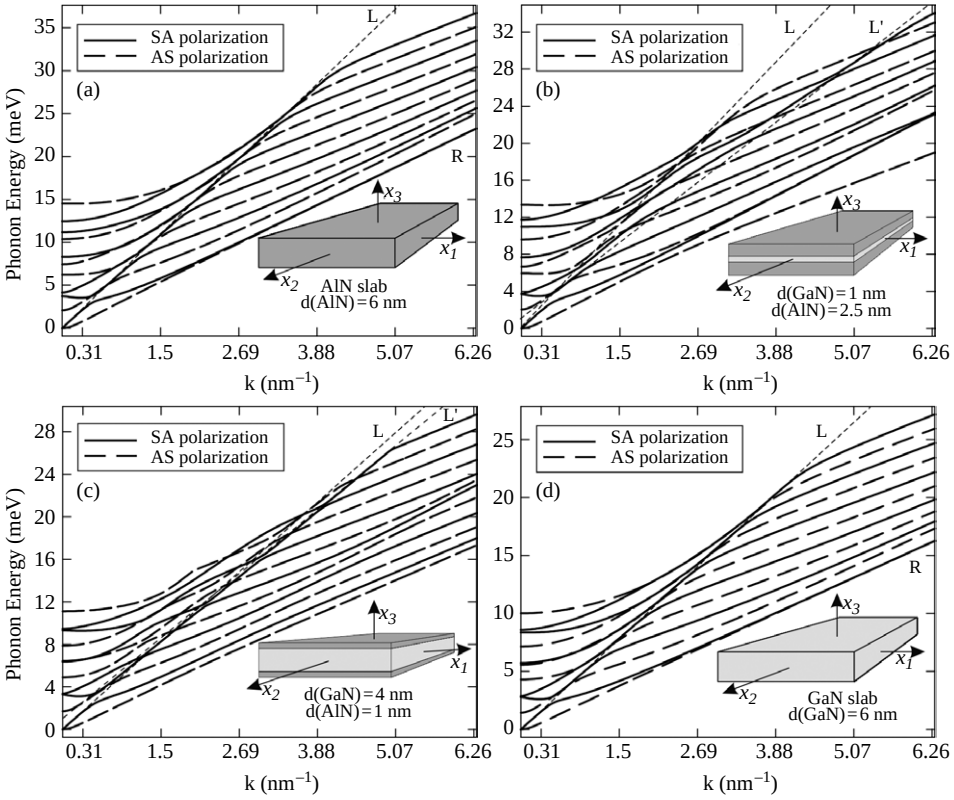

Fig. 4. Energy dispersion of the SA and AS acoustic phonon modes. The results are shown for (a) the 6 nm width AlN slab and (b) the heterostructure type I with the cladding layer thickness $d_1 = d_3 = 2.5$ nm and the core layer thickness $d_2 = 1.0$ nm; as well as for (c) the heterostructure type II with the cladding layer thickness $d_1 = d_3 = 1.0$ nm and the core layer thickness $d_2 = 4.0$ nm and (d) the 6 nm width GaN slab. Inset shows the geometry of the slab and three-layered structure.

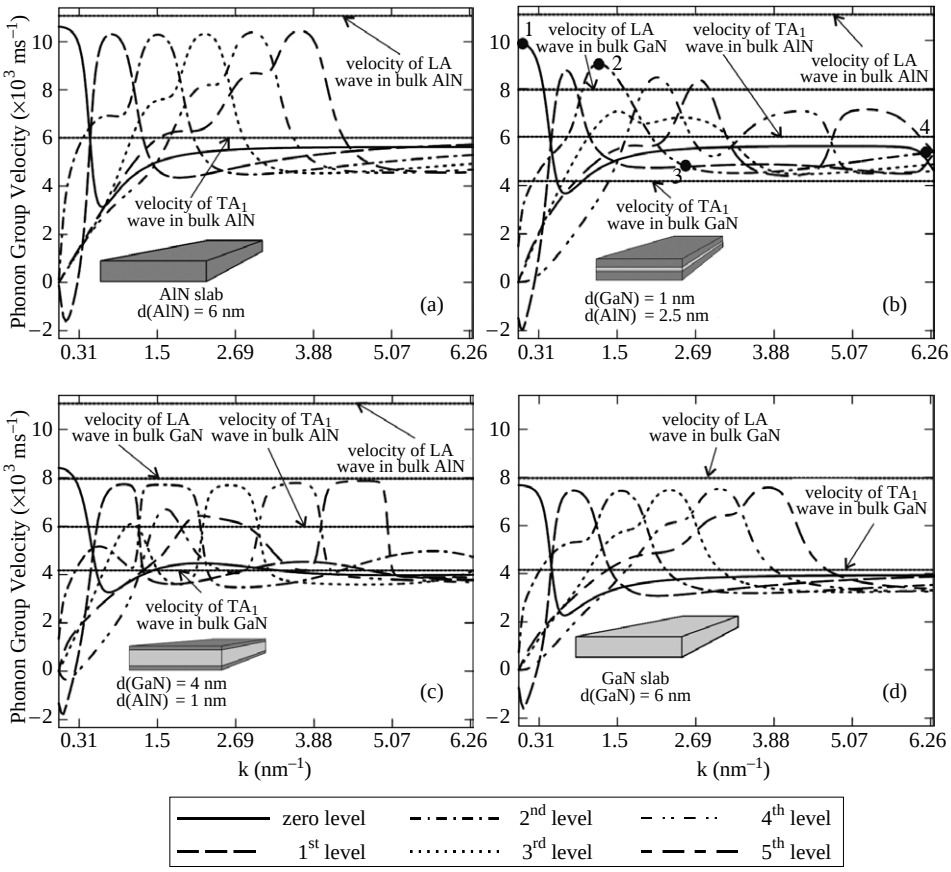

Fig. 5. Phonon group velocities as the functions of the phonon wavevector for the SA acoustic phonon modes. The sizes of the slabs (a, d) and heterostructures (b, c) are same as in the previous Fig. 3(a–d).

In the limit of large phonon wavevectors k, the group velocity is the same for almost all modes. Its value is slightly lower that the bulk transverse sound velocity $v^{\mathrm{TA}_1}(\mathrm{AlN})$ (see Fig. 4(a)) and $v^{\mathrm{TA}_1}(\mathrm{GaN})$ (see Fig. 4(d)) due to the phonon confinement or "slab" effect. Here v^{TA_1} is the velocity of the transverse acoustic wave propagating along the X_1 axis and polarized along the reference axis (TA_1 polarized waves). The appearance of line L in the phonon energy dispersion for a simple slab is explained by mixing of waves with potential and solenoidal polarizations (LA and TA_1 polarizations in a bulk limit).

Fig. 4(c) presents results for the structure, which we refer to as structure type-II to identify that it consists of a "thick" core layer and "thin" cladding layers. In the three-layered heterostructures of type-I and type-II one can spot two characteristic lines (L and L′) shown in Fig. 4(b, c). Correspondingly, the group velocity curves in Fig. 5(b, c) display two different maxima. The sequence of the higher maxima corresponds to the line L with the slope $v_{\mathrm{L}} \approx v^{\mathrm{LA}}(\mathrm{AlN})$ while the sequence of the lower maxima corresponds to the

line L′ with the slope $v_{\mathrm{L}} \approx v^{\mathrm{LA}}(\mathrm{GaN})$. The existence of two lines (L and L′) in the phonon energy spectra is a result of wave mixing and hybridization in the heterostructure. Both lines are clearly seen in Fig. 4(b) for the type-I heterostructure while for the type-II heterostructure (Fig. 4(c)) the line L is defined by the initial segment of the mode $n = 0$ curve only. The reduction of the AlN-like modes in the type-II heterostructure is explained by a much thicker GaN core layer, which leads to the decrease of the group velocities of all phonon modes. The lines L and L′ divide the phonon dispersion into three distinctively different regions (see Fig. 4(b, c)): (i) region of the strong phonon size quantization for small k and to the left from line L; (ii) region with abrupt change of dispersion characteristics between lines L and L′, and (iii) region to the right from line L′ with low-frequency modes and with group velocities approaching the low bulk velocity $v^{\mathrm{TA}_1}(\mathrm{AlN})$ (see Fig. 4(b)) and $v^{\mathrm{TA}_1}(\mathrm{GaN})$ (see Fig. 4(c)). One can notice that AS and SA modes display more the individual layer properties rather than the averaged properties of the heterostructure, although the narrow region between lines L and L′ can be thought of as the region having properties, which is the average of the core and cladding layer properties. Another observation is that the Rayleigh line (R) [14], which is present in Fig. 4(a, d) for simple slabs does not appear in the heterostructure energy spectra (Fig. 4(b, c)).

The behavior of the phonon dispersion and group velocity is determined by the specifics of the distribution of the displacement vectors in the layers of the heterostructure. As an example, in Fig. 6(a–d) we show the components of the displacement vectors $u^{\mathrm{SA}}_{1,n}(x_3)$ (solid line) and $u^{\mathrm{SA}}_{3,n}(x_3)$ (dashed line) for the type-I structure. The chosen modes n and values of the phonon wavevector k are the following: $n = 0$, $k = 0.05\ \mathrm{nm}^{-1}$ (a); $n = 2$, $k = 1.256\ \mathrm{nm}^{-1}$ (b); $n = 2$, $k = 1.44\ \mathrm{nm}^{-1}$ (c); and $n = 2$, $k = 6.28\ \mathrm{nm}^{-1}$ (d). These four cases (a–d) shown in Fig. 6 correspond to the points on the group velocity plot in Fig. 5(b) indicated by filled circles. One can see from Fig. 6(a) that the amplitude $u^{\mathrm{SA}}_{1,n=0}(x_3)$ is constant in all layers of the heterostructure. The latter together with the fact that the combined thickness of the cladding layers is much larger than the thickness of the core layer explain the (AlN, LA)-like nature of this mode. The mode $n = 2$ at $k = 1.256\ \mathrm{nm}^{-1}$ (see Fig. 6(b)) is also (AlN, LA)-like since the amplitude $u^{\mathrm{SA}}_{1,n=2}(x_3)$ is distributed predominantly in the cladding layer. The contributions of different polarizations, e.g. potential, solenoidal, to the displacement vector $\vec{U}$ can be obtained by calculating div $\vec{U}$ and curl $\vec{U}$. Such calculation for mode $n = 0$ at $k = 0.05\ \mathrm{nm}^{-1}$ demonstrates that this mode is LA bulk-like, which is in complete agreement with Fig. 4(b) since curl $\vec{U} = 0$ and div $\vec{U} \neq 0$ for this case.

For calculation of different macroscopic characteristics of nanostructures, such as thermal and electrical conductivity, heat capacity, etc., it is required to know the spectral density of the phonon mode distribution, e.g. phonon density of states. In the considered plane structures with thin core and cladding layers the phonon wavevector is two dimensional. Thus, the phonon density of states for each of the SA, AS or shear polarizations with given mode number n is defined by the expression

$$f_n^{\mathrm{SA,AS,sh}}(\omega) = \frac{1}{2\pi} k_n^{\mathrm{SA,AS,sh}}(\omega) \frac{\mathrm{d}k_n^{\mathrm{SA,AS,sh}}(\omega)}{\mathrm{d}\omega}. \tag{12}$$

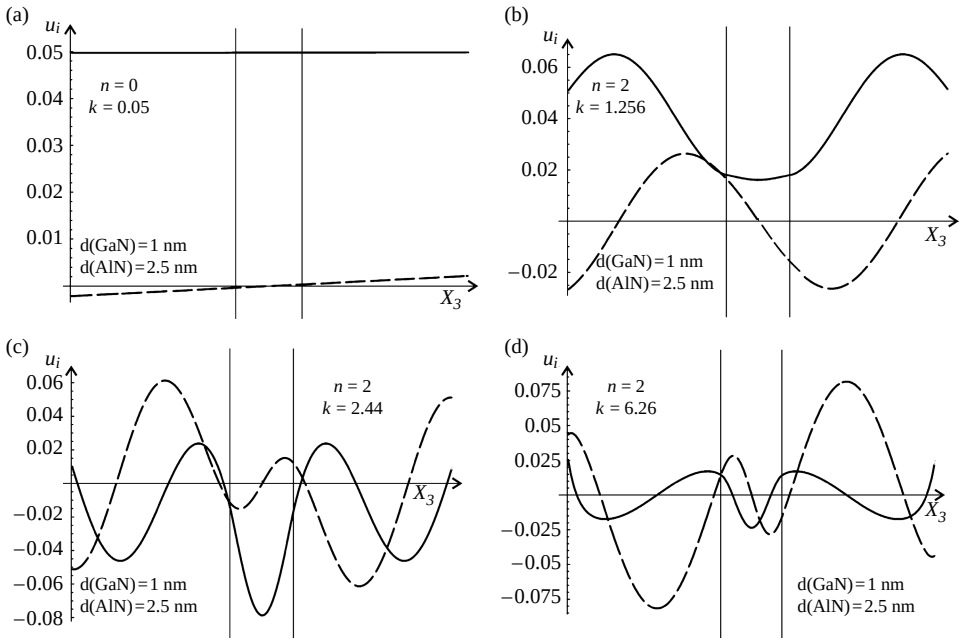

Fig. 6. Components of the displacement vector u_1 (solid line) and u_3 (dashed line) of SA phonon modes as the functions of the coordinate x_3. The results are shown for four phonon modes: (a) $n = 0$, $k = 0.05$ nm^{-1}; (b) $n = 2$, $k = 1.256$ nm^{-1}; (c) $n = 2$, $k = 2.44$ nm^{-1}; (d) $n = 2$, $k = 6.26$ nm^{-1}.

The total phonon density of states for all polarizations is obtained by a summation over all n

$$F^{\mathrm{SA,AS,sh}}(\omega) = \sum_n f_n^{\mathrm{SA,AS,sh}}(\omega). \tag{13}$$

For the type-I and type-II three-layered structures the total phonon density of states $F^{\mathrm{SA,AS,sh}}(\omega)$ is presented in Fig. 7. For comparison, the total phonon density of states in simple GaN and AlN slabs is also shown. The oscillatory behavior of the density of states functions in the three-layered structure for each polarization is a manifestation of the phonon mode quantization and their *quasi*-optical nature ($\omega(k = 0) \neq 0$). Local steps in the density of states correspond to the onset of new phonon branches when their cut-off frequencies are reached. Altering the phonon density of states in the three-layered structure for low frequencies can lead to significant change in the electron–phonon scattering rates particularly for low temperatures.

The average phonon group velocity is an important characteristic that determines, for example, the lattice thermal conductivity of bulk semiconductors or nanostructures [2, 10]. We calculate the average phonon group velocity for each polarization as a velocity of a wavepacket with the modes populated in accordance with the Bose–Einstein distribution function

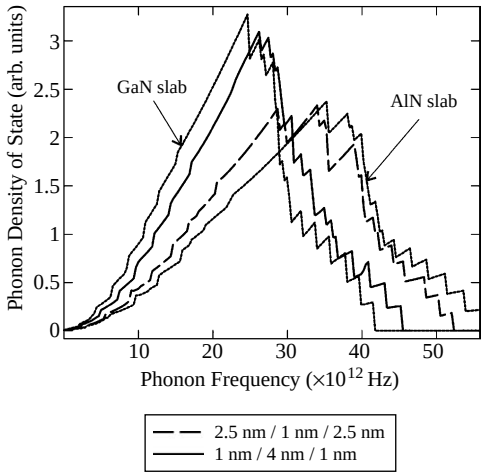

Fig. 7. Total phonon density of states as the function of the phonon frequency for the GaN slab, for the AlN slab and for type-I and type-II heterostructures. The structures sizes are shown in the figure.

$$\overline{v}^{\mathrm{SA,AS,sh}}(T) = \frac{\int_{\omega_{n\min}}^{\omega_{n\max}} \mathrm{d}\omega n\left(\frac{\hbar\omega}{T}\right) \sum_n v_n^{\mathrm{SA,AS,sh}}(\omega)\, f_n^{\mathrm{SA,AS,sh}}(\omega)}{\sum_n f_n^{\mathrm{SA,AS,sh}}(\omega)}, \tag{14}$$

where $n(\hbar\omega/T)$ is the Bose–Einstein equilibrium distribution function for phonons. Fig. 8 shows the average phonon group velocity $\overline{v}^{\mathrm{SA,AS,sh}}(T)$. The results are presented for all three phonon polarizations: SA (solid line), AS (dotted line), and shear (dashed line). In type-I and type-II heterostructures, the average velocity of the thermal phonon current is considerably higher than that in the GaN slab, which is explained by the influence of the AlN cladding. For example, in the type-I structure at $T = 300$ K the following ratios for the group velocities were found $v^{\mathrm{SA}}(\text{type-I})/v^{\mathrm{SA}}(\text{GaN}) = 1.35$, $v^{\mathrm{AS}}(\text{type-I})/v^{\mathrm{AS}}(\text{GaN}) = 1.29$, and $v^{\mathrm{sh}}(\text{type-I})/v^{\mathrm{sh}}(\text{GaN}) = 1.26$.

Our results demonstrate that it is possible to tune the velocity of the phonon flux in a semiconductor quantum well layer over a wide range of values. By proper selection of the material and width of the cladding layers one can either considerably increase or decrease the phonon group velocity in the core quantum well layer. This is an important capability for heat transport. Indeed, thermal conductivity coefficient K_T can be approximately written as $K_T \sim C_V V \Lambda$, where C_V is the specific heat per unit volume, Λ is the average phonon mean free path, and $V = \sum \overline{v}^{\mathrm{SA,AS,sh}}$ is the phonon group velocity averaged over all polarizations and directions. For small wavevectors in bulk material this velocity coincides with the sound velocity. Thus, the thermal conductivity coefficient depends on the phonon velocity implicitly and through the phonon mean free path Λ, which is a strong function of the phonon group velocity. In the next subsection we examine the range over which the group velocity can be changed by combining “hard” and “soft” materials.

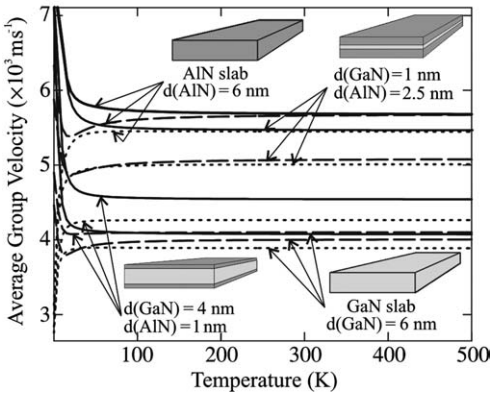

Fig. 8. Population averaged phonon group velocities as the functions of temperature for the AlN, GaN slabs and type-I and type-II heterostructures. The results are shown for SA (solid line), AS (dotted line), and shear (dashed line) phonon polarizations.

3.2. Three-layered heterostructures with the "soft" and "hard" cladding layers

In order to demonstrate a possibility of strong modification of the phonon group velocity and, correspondingly the heat current in confined structures, by choosing cladding layers, we consider two new structures. Structure type-III is a GaN layer embedded in some "soft" plastic material: plastic/GaN/plastic. We consider that the GaN layer is very thin, on the order of 1 nm, so that it can be considered as a quantum well. The chemical structure of the plastic material used for the cladding layers is not essential for our analysis. We only assume that the sound velocity in bulk plastic is 2000 m s^{-1}, and mass density is 1 g sm^{-3}. The chosen values of these parameters correspond to those of a large number of materials used in practice [24]. Another structure under consideration, type-IV, consists of a very thin layer of plastic embedded within two layers of "hard" material such as sapphire: Al_2O_3 /plastic/ Al_2O_3. We carry out simulations for these two new structures following the procedure outlines above.

In Figs 9(a, b) and 10(a, b) we show the dispersion relations $\hbar\omega(k)$ for SA modes in structure type-III (the thickness of the core GaN layer is fixed at 1 nm while the thickness of each of the two cladding layers spans the values 3 and 10 nm) and in structure type-IV (the thickness of the core plastic layer is fixed at 1 nm while the thickness of the Al_2O_3 cladding layers spans the values 3 and 10 nm). In Fig. 9(a) the slope of the line L is approximately equal to the velocity of LA phonons in plastic $v_L \approx v^{LA}(Pl)$ while the slope of the dispersion L branches $\hbar\omega^{SA}(k)$ to the right from this line approaches TA phonon velocity in plastic $v^{TA}(Pl)$. The GaN core contribution is suppressed in this type of structure since the plastic cladding effect and the slab-like phonon confinement effect both lead to the same dispersion flattening. Therefore the type-III heterostructure becomes effectively plastic slab-like. The "soft" cladding of the GaN thin films results in strong phonon deceleration in such a structure. The increase of the width of the plastic cladding does not change much in this picture.

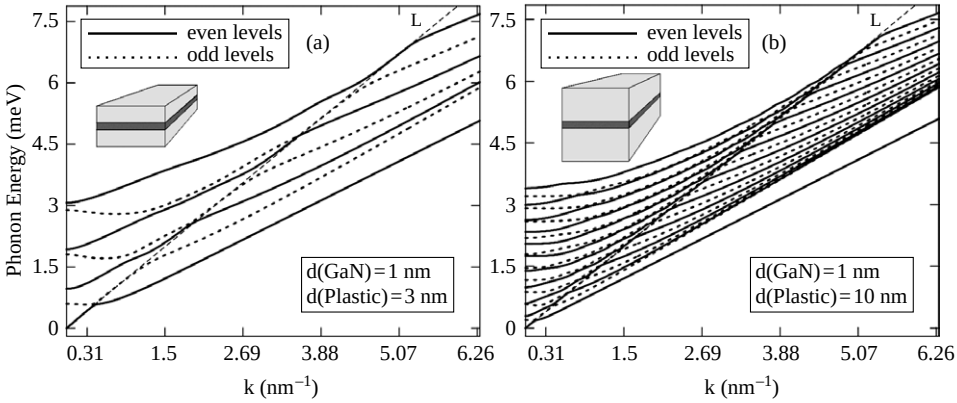

Fig. 9. Energy dispersion of the SA acoustic phonon modes for type III heterostructures. The results are shown for (a) the heterostructure with the cladding layer thickness $d_1 = d_3 = 3.0$ nm and the core layer thickness $d_2 = 1.0$ nm; as well as for (b) the heterostructure with the cladding layer thickness $d_1 = d_3 = 10.0$ nm and the core layer thickness $d_2 = 1.0$ nm.

Fig. 10(a, b) demonstrates the accelerating action of Al_2O_3 claddings on phonon velocity in the type-IV heterostructure with the plastic core layer of thickness $d = 1$ nm. In this case, the phonon confinement "slab effect" and the influence of the Al_2O_3 cladding act in opposite directions and the inhomogeneous nature of the heterostructure is strongly manifested. The type-IV heterostructure does not become slab-like even with very thick Al_2O_3 cladding layers. In Fig. 10(b) one can see both characteristic lines (L and L′) with the slope equal to $v^{LA}(Al_2O_3)$ and $v^{TA_1}(Al_2O_3)$, correspondingly. An intermediate region between these lines is characterized by abrupt and multiple changes in phonon velocity in the interval of values ($v^{TA}(Pl)$, $v^{LA}(Al_2O_3)$). To the right from line L′ there is a region of low-velocity phonons ((plastic, TA)-like modes). With increasing width of the cladding layers the intermediate region extends and the number of "fast" phonon modes increases. At the same time, the "hard" cladding layers do not completely overcome the "slowness" of the core layer. Therefore, the effect of the phonon acceleration in the type-IV heterostructure is weaker than the effect of deceleration in the type-III heterostructure.

Quantitatively, the effect of phonon deceleration and acceleration, e.g. change in the average group velocities, in heterostructures can be illustrated with the following ratios, which correspond to several points in Fig. 11. In the type-III heterostructure (3/1/3 nm) at the temperature $T = 20$ K the ratio of the average phonon group velocity in the heterostructure to the group velocity in the slab is $v(\text{hetero})/v(\text{GaN slab}) = 0.17$ (see Figs 9(a) and 11). In the type-III structure with dimensions 10/1/10 nm, the ratio is $v(\text{hetero})/v(\text{GaN slab}) = 0.16$ (see Figs 9(b) and 11). At room temperature ($T = 300$ K) the ratio for both heterostructures is the same and equal to 0.26. The latter is a factor of 3.84 decrease in the average phonon group velocity in the three-layered heterostructure compared to GaN slab (thin film) due to the presence of "soft" cladding layers. One should point out here that the average phonon group velocity in the slab (ultra-thin film) is already smaller than the phonon (sound) velocity in the corresponding bulk. In the

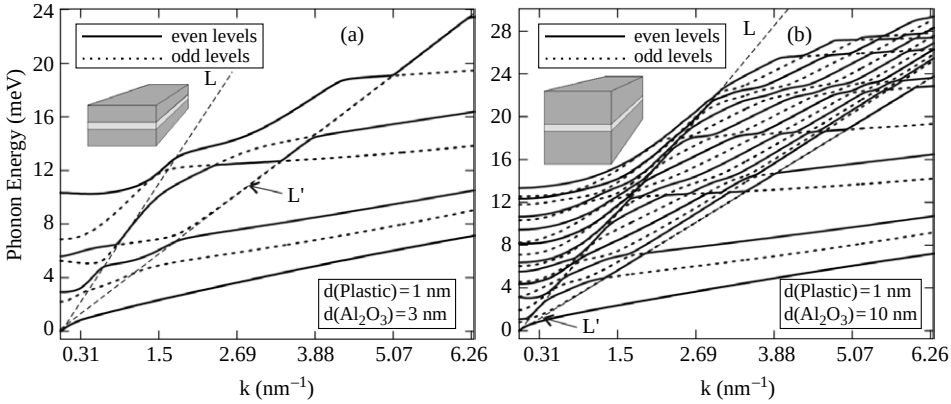

Fig. 10. Energy dispersion of the SA acoustic phonon modes for type IV heterostructures. The results are shown for (a) the heterostructure with the cladding layer thickness $d_1 = d_3 = 3.0$ nm and the core layer thickness $d_2 = 1.0$ nm; as well as for (b) the heterostructure with the cladding layer thickness $d_1 = d_3 = 10.0$ nm and the core layer thickness $d_2 = 1.0$ nm.

type-IV heterostructure (3/1/3 nm) at the temperature $T = 20$ K the ratio of the average phonon group velocity in the heterostructure to the group velocity in the slab is $v(\text{hetero})/v(\text{plastic slab}) = 1.06$ (see Figs 8(a) and 10). In the type-IV structure with dimensions 10/1/10 nm, the ratio is $v(\text{hetero})/v(\text{plastic slab}) = 1.4$ (see Figs 8(b) and 10). At room temperature ($T = 300$ K) the ratios for these two heterostructures are 1.36 and 2.36, correspondingly.

It is also important to compare the averaged phonon group velocity in the three-layered heterostructures and in the corresponding bulk material. For example, in the type-IV structures, the average velocity of the thermal phonon current in the core layer can be made higher than that in the corresponding bulk material. Such a velocity increase is due to the influence of the “hard” and “thick” cladding layer. In the type-II structure (“thin” cladding layer, “thick” core layer) the average velocity in the core GaN layer is lower than that in the bulk GaN. The latter is due to the fact that the effect of the barrier here is less pronounced and the velocity change in the core GaN layer is mostly defined by the phonon mode quantization and flattening of the polarization branches (see Figs 1 and 2). This is in line with the prediction of the significant decrease of the phonon group velocity in free standing quantum wells (or slabs) [2] and nanowires [10].

4. Conclusions

We have theoretically investigated phonon dispersion and phonon group velocity in AlN/GaN/AlN and other related heterostructures. The focus of this study was on understanding the effect of the cladding (barrier) layers on the population averaged phonon group velocity in such structures. It has been shown that by proper selection of the cladding material parameters and its thickness, one can make the group velocity in the core layer of such heterostructures either larger or smaller than in the corresponding slab and bulk.

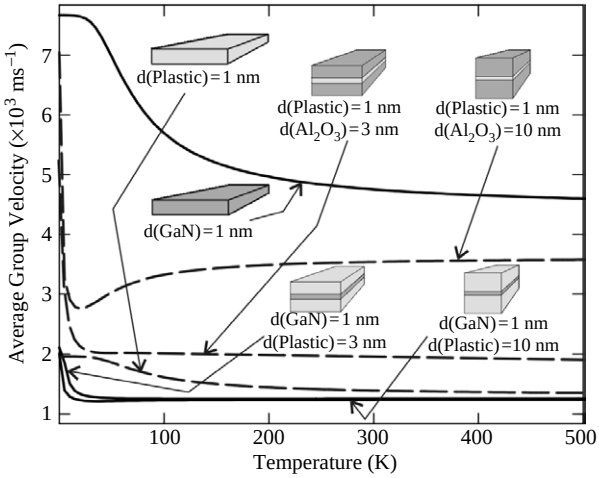

Fig. 11. Population averaged phonon group velocities as the functions of temperature for the plastic and GaN slabs and for the type-III and type-IV heterostructures. The results are shown for the SA phonon polarization and two different values of the cladding layer thickness.

For example, it was demonstrated that in a structure that consists of a 1 nm thick GaN core layer embedded in 2.5 nm thick AlN cladding layers, the population averaged phonon group velocity at 300 K is about 30% higher than in the GaN slab. The fact that the phonon group velocity in heterostructures can be modulated bears important consequences for phonon heat transport and thermal management of electronic devices.

Acknowledgements

The work in UCR was supported in part by ONR project N00014-02-1-0352 and NSF CAREER Award to A.A.B. The work in SUM was supported in part by the U.S. Civil Research and Development Foundation project MP2-3044.

References

[1] C.M. Bhandari, D.M. Rowe, Thermal Conduction in Semiconductors, John Wiley & Sons, New York, 1988.
[2] A. Balandin, K.L. Wang, Phys. Rev. B 58 (1998) 1544.
[3] T. Klitsner, R.O. Pohl, Phys. Rev. B 36 (1987) 6551.
[4] U. Bockelmann, Phys. Rev. B 50 (1994) 17271.
[5] H. Benisty, Phys. Rev. B 51 (1995) 13281.
[6] M. Dur, A.D. Gunther, D. Vasileska, S.M. Goodnik, Nanotechnology 10 (1999) 142.
[7] H. Benisty, C.M. Sotomayor-Torres, C. Weisbuh, Phys. Rev. B 44 (1991) 10945.
[8] H. Noguchi, J.P. Leburton, H. Sakaki, Phys. Rev. B 47 (1993) 15593.
[9] Y. Lyanda-Geller, J.P. Leburton, Semicond. Sci. Technol. 15 (2000) 700.
[10] J. Zou, A. Balandin, J. Appl. Phys. 89 (2001) 2932.
[11] S. Volz, D. Lemonier, Phys. Low-Dim. Struct. 5–6 (2000) 91.
[12] X. Lu, J.H. Chu, W.Z. Shen, J. Appl. Phys. 93 (2003) 1219.
[13] W.P. Meson (Ed.), Physical Acoustic, part A, vol. I. Academic Press, New York, 1964.

[14] S.M. Rytov, Akust. Zh. 2 (1956) 71 (Sov. Phys.—Acoust. 2 (1956) 67).
[15] C. Colvard, T.A. Gant, M.V. Klein, R. Merlin, R. Fisher, H. Morkoc, A.C. Gossard, Phys. Rev. B 31 (1985) 2080.
[16] N. Bannov, V. Aristov, V. Mitin, M.A. Stroscio, Phys. Rev. B 51 (1995) 9930.
[17] A. Svizhenko, A. Balandin, S. Bandyopadhyay, M.A. Stroscio, Phys. Rev. B 57 (1998) 4687.
[18] M.A. Stroscio, K.W. Kim, S.G. Yu, A. Ballato, J. Appl. Phys. 76 (1994) 4670.
[19] O.L. Lazarenkova, A.A. Balandin, Phys. Rev. B 66 (2002) 245319.
[20] O. Stier, D. Bimberg, Phys. Rev. B 55 (1997) 7726.
[21] I. Vurgaftman, J.R. Meyer, L.R. Ram-Mohan, J. Appl. Phys. 89 (2001) 5815.
[22] V. Bougrov, M. Levinshtein, S.L. Rumyantsev, A. Zubrilov, Properties of Advanced Semiconductor Materials, M.E. Levinshtein, S.L. Rumyantsev, M.S. Shur (Eds.), John Wiley & Sons, Inc., New York, 2001.
[23] See for example at https://classes.yale.edu/eeng418a/classnotes/EE418_c13.pdf.
[24] See for example at http://www.ondacorp.com/tables/plastics.htm.